 

PACS numbers: 81.20.Fw; 82.70.Dd; 61.46.Df; 42.65.Re
DOI: 10.1070/QE2015v045n05ABEH015760

# Photofragmentation of colloidal solutions of gold nanoparticles under femtosecond laser pulses in IR and visible ranges

P.A. Danilov, D.A. Zayarnyi, A.A. Ionin, S.I. Kudryashov, V.N. Lednev, S.V. Makarov, S.M. Pershin, A.A. Rudenko, I.N. Saraeva, V.I. Yurovskikh

*Abstract.* **The specific features of photofragmentation of sols of gold nanoparticles under focused femtosecond laser pulses in IR (1030 nm) and visible (515 nm) ranges is experimentally investigated. A high photofragmentation efficiency of nanoparticles in the waist of a pulsed laser beam in the visible range (at moderate radiation scattering) is demonstrated; this efficiency is related to the excitation of plasmon resonance in nanoparticles on the blue shoulder of its spectrum, in contrast to the regime of very weak photofragmentation in an IR-laser field of comparable intensity. Possible mechanisms of femtosecond laser photofragmentation of gold nanoparticles are discussed.**

***Keywords:*** *gold nanoparticle sols, femtosecond laser pulses in IR and visible ranges, plasmon resonance, extinction, absorption, scattering.*

## 1. Introduction

Femtosecond laser ablation of the surface of various materials in a liquid is a universal method for preparing colloidal solutions of chemically pure nanoparticles without any traces of precursors [1]. At the same time, in contrast to chemical methods for forming colloidal solutions of nanoparticles, nanoparticles obtained by laser ablation in liquids have generally a rather large spread in size [2, 3].

One of the most popular methods for homogenising polydisperse colloidal solutions of nanoparticles is their secondary multipulsed irradiation by ultrashort laser pulses (USLPs) in order to fragmentate nanoparticles [4]. In contrast to the effect of short, i.e., (sub)nanosecond and submicrosecond, laser pulses, the secondary effect of USLPs is a more controllable process, because incorporation of laser energy into nanoparticles occurs virtually instantaneously during their electron–phonon relaxation; subsequent heating of nanoparticles leads to water boiling on their surface [5]. The physics of nanoparticle photofragmentation was investigated in a number of studies [6, 7]; however, liquids are characterised by certain specificity of thermal and hydrodynamic processes of interaction between nanoparticles and USLPs [8]. At the same time, even the most systematic previous studies [9, 10] disregarded the very important effect of filamentation by USLPs in liquids as transparent dielectric media at energies above several microjoules and simultaneous spectral USLP conversion as a result of generation of a broadband supercontinuum [11, 12]. This conversion is often related to USLP splitting into several shorter subpulses [13], which can interact with nanoparticles in a quite a different way, for example, via Coulomb explosion [7]. As a result, in some cases (especially for IR USLPs), photofragmentation of nanoparticles in the USLP filamentation regime was accompanied by photolysis with unexpectedly high efficiency [9, 10], despite the fact that IR scattering from nanoparticles is more preferred [14]. Correspondingly, the spectral features of nanoparticle photofragmentation in liquids under USLPs remain insufficiently investigated.

In this paper we report the results of experimental study of the spectral features of photofragmentation of gold nanoparticle sols under focused femtosecond laser pulses in IR (1030 nm) and visible (515 nm) ranges, both in the vicinity of the plasmon resonance of nanoparticles and far from it. The experiments were performed in the regime of filamentation-free propagation of USLPs, which made it possible to study photofragmentation under controlled conditions of laser irradiation. Possible mechanisms of nanoparticle photofragmentation are discussed with allowance for the obtained dependence of the nanoparticle size on the exposure time of colloidal solution.

## 2. Experimental

A solution of nanoparticles was prepared by ablation of a gold target ingot (purity of 99.99%) with an optical-quality surface in a Petri dish under a thin (~1 mm) layer of isopropyl alcohol, using USLPs generated by a laser (Satsuma, Amplitude Systems) with a centre wavelength of ~1030 nm, pulse FWHM ~0.3 ps and energy up to 10 μJ in the $TEM_{00}$ mode; the laser beam was focused into a spot with a radius $R_{1/e} \approx 10$ μm. The laser active medium was an ytterbium-doped fibre. The target surface was irradiated in the scan regime at a pulse repetition rate of ~10 kHz and scan rate of

**P.A. Danilov, S.I. Kudryashov, V.I. Yurovskikh** P.N. Lebedev Physics Institute, Russian Academy of Sciences, Leninsky prosp. 53, 119991 Moscow, Russia; National Research Nuclear University 'MEPhI', Kashirskoe sh. 31, 115409 Moscow, Russia; e-mail: sikudr@sci.lebedev.ru;
**D.A. Zayarnyi, A.A. Ionin, A.A. Rudenko, I.N. Saraeva** P.N. Lebedev Physics Institute, Russian Academy of Sciences, Leninsky prosp. 53, 119991 Moscow, Russia;
**V.N. Lednev, S.M. Pershin** A.M. Prokhorov General Physics Institute, Russian Academy of Sciences, ul. Vavilova 38, 119991 Moscow, Russia;
**S.V. Makarov** P.N. Lebedev Physics Institute, Russian Academy of Sciences, Leninsky prosp. 53, 119991 Moscow, Russia; ITMO University, Kronverkskii prosp. 49, 197101 St. Petersburg, Russia; e-mail: makarov_sergey_vl@mail.ru

Received 29 January 2015; revision received 6 February 2015
Kvantovaya Elektronika **45** (5) 472–476 (2015)
Translated by Yu.P. Sin'kov

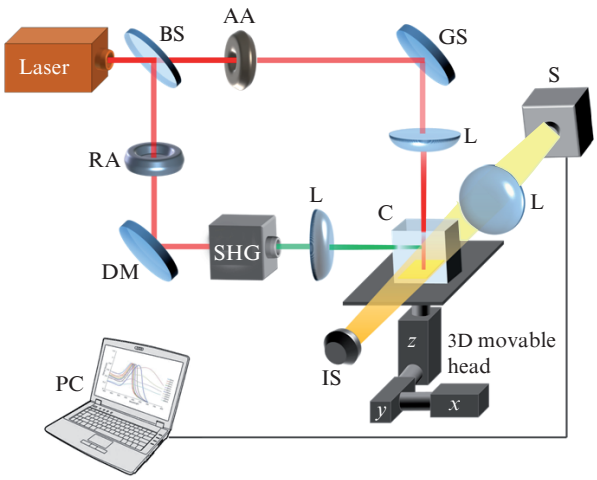


**Figure 1.** Schematic of the experiment on laser generation and fragmentation of nanoparticles using optical transmission spectroscopy in situ: (BS) beam splitter; (AA, RA) acousto-optic and reflection attenuators; (DM) dielectric mirrors; (GS) galvanometer scanner; (SHG) second-harmonic generator; (S) spectrometer with a CCD array; (IS) illumination source; (C) cell with a target; (L) focusing lenses; (PC) personal computer for controlling experiment and collecting data.

~50 mm $s^{-1}$, which was implemented using an ATEKO galvanometer scanner (Fig. 1).

Fragmentation of the produced colloidal solution of nanoparticles in isopropyl alcohol (volume ~2 mL) occurred under exposure to multipulse radiation of the same laser, focused inside a quartz cell 1 cm wide by a lens with a focal length of ~5.5 cm, both at the fundamental wavelength (1030 nm) and at the second-harmonic wavelength (515 nm); the pulse width was ~0.2 ps, energy up to 4 μJ (515 nm) or 10 μJ (1030 nm) in the $TEM_{00}$ mode. The repetition rate of second-harmonic pulses was varied in the range of 10–500 kHz, and the irradiation time corresponded to the number of pulses $N = 10^5$–$10^9$, which is necessary (in the small focal volume) for single exposure of the entire volume of the colloidal nanoparticle solution. During photofragmentation, the cell was cyclically moved upward and downward on a computer-controlled motorised stage with a velocity of 0.8 mm $s^{-1}$ in order to mix the solution. All nanoparticle sols were investigated by optical transmission spectroscopy in a quartz cell with an optical path length of ~1 cm. To analyse the final size distribution of gold nanoparticles, they were deposited on an atomically smooth silicon plate and visualised using a JEOL 7001F scanning electron microscope (SEM).

## 3. Experimental results

Colloidal solutions of gold nanoparticles were prepared by laser ablation of the surface of a gold target placed in isopropyl alcohol, using IR USLPs with energy density $F \approx 2.5$ J $cm^{-2}$ in the multipulse regime. The ablation effect gives rise to a fairly wide distribution of nanoparticle sizes (diameters) $d$: from 5 to 100 nm (Fig. 2a), with a maximum in the range of $d = 15$–$30$ nm (Fig. 2c). The observed inhomogeneity of the nanoparticle ensemble is apparently related to the hydrodynamic spread of supercritical fluid [15] (the spallation ablation threshold for this target in air is ~1.7 J $cm^{-2}$), which is accompanied by not only intense escape of vapour–drop

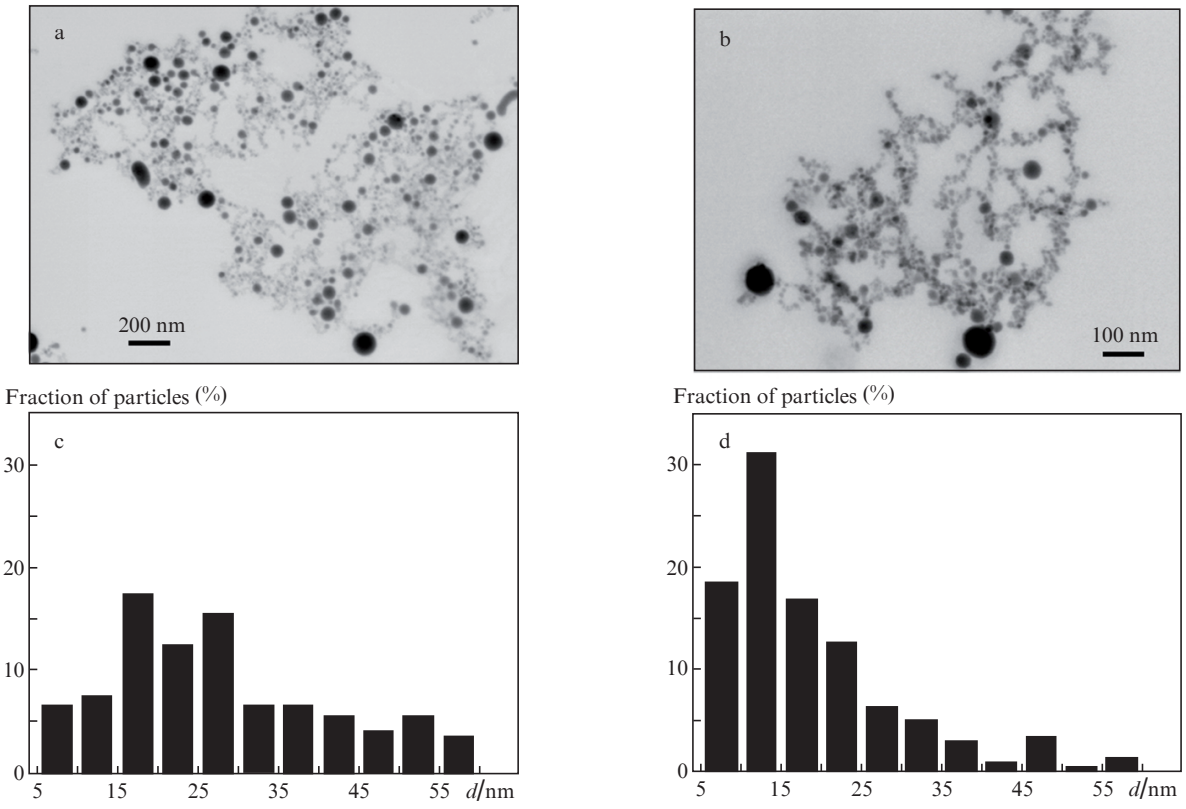


**Figure 2.** (a, b) SEM images of gold nanoparticles and (c, d) the corresponding size distributions of nanoparticles (a, c) before and (b, d) after irradiation at $\lambda = 515$ nm for a number of pulses $N \approx 10^7$.

mixture in the form of small nanoparticles from the surface but also possible development of hydrodynamic instabilities with formation of jets and their detachment in the form of relatively large nanoparticles [16]. A study of the extinction spectra of the colloidal solutions of gold nanoparticles showed that, after their formation, the peak of extinction coefficient $\alpha_m$ has an FWHM ~125 nm, and the position of this peak corresponds to the wavelength $\lambda \approx 555$ nm (Figs 3a, 3c).

Photofragmentation of colloidal solutions of nanoparticles by laser radiation with $\lambda = 515$ nm after irradiation by $10^7$ pulses with energy of ~3.5 μJ (this value is much below the filamentation threshold of USLPs in isopropyl alcohol, which is related to the spectral broadening of transmitted pulse) leads to a significant size redistribution of nanoparticles. One can see that the fraction of large nanoparticles becomes smaller (Fig. 2d), while the number of smallest nanoparticles increases (with a simultaneous shift of their distribution peak to the range of diameters $d = 10–15$ nm) by a factor of about two in comparison with the unirradiated solution. A similar effect is observed in extinction spectra: the peak of extinction coefficient $\alpha_m$ is gradually blue-shifted with an increase in the number of pulses $N$ to $\lambda_{max} \approx 530$ nm; this value does not change with a further increase in $N$ (Fig. 3b). The extinction band width $\Delta\lambda$ decreases with an increase in $N$ to ~85 nm (Fig. 3b). It is noteworthy that the obtained colloidal solutions of fragmented nanoparticles are characterised by much higher stability in comparison with the initial colloidal solutions of nonfragmented nanoparticles: the initial solution becomes colourless under normal conditions, and a precipitate is formed on the walls of a plastic container after about 24 h, whereas a fragmented nanoparticle solution retains its optical density at room temperature during almost two weeks.

At the same time, at much higher (by a factor of 2.5) energy of IR pulses (~9 μJ, which is also below the filamentation threshold in isopropyl alcohol) and comparable number of USLPs ($N \approx 10^9$), IR photofragmentation of colloidal solutions did not lead to any significant changes in the size distribution of nanoparticles. Extinction spectra confirm that IR irradiation did not shift the maximum of the extinction band or cause its narrowing (Figs 3c, 3d).

## 4. Discussion

SEM images of gold nanoparticles (Fig. 2) show that these objects have a spherical shape and sizes much smaller than the light wavelengths in the range under consideration (450–700 nm). Correspondingly, the absorption and scattering coefficients of these particles can be calculated within the quasi-static approximation [14]:

$$\sigma_{abs} = 4\pi k_2 \mathrm{Im}\alpha, \quad (1)$$

$$\sigma_{scat} = \frac{8\pi}{3} k_2^4 |\alpha|^2, \quad (2)$$

where $k_2$ is the wave number of radiation in the medium surrounding a nanoparticle;

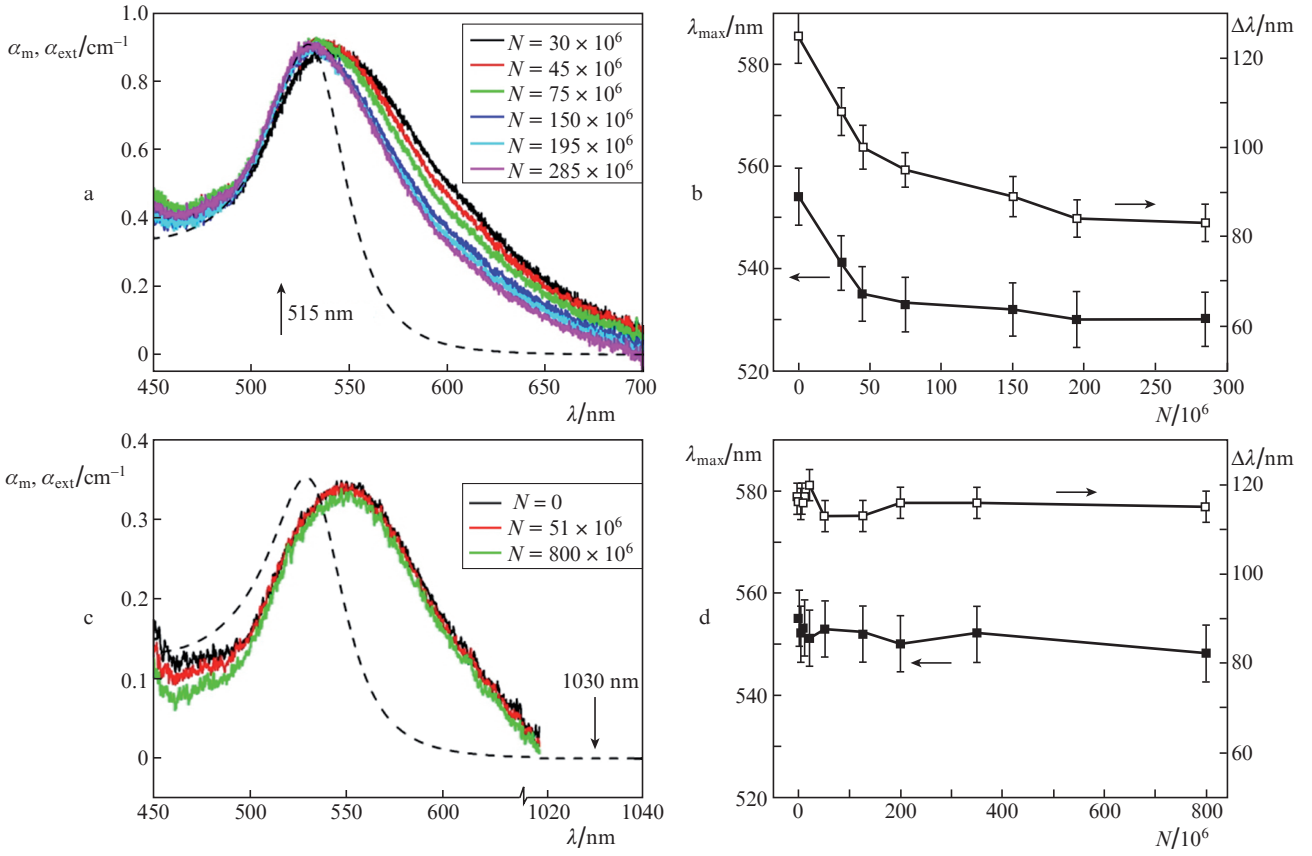


**Figure 3.** (Colour online) (a, c) Experimental spectra of extinction coefficient $\alpha_m(\lambda)$ for solutions of nanoparticles in isopropyl alcohol, irradiated by different numbers $N$ of USLPs at $\lambda$ = (a) 515 and (c) 1030 nm (the dashed curves are the calculated spectra $\alpha_{ext}$ for monodisperse particles 10 nm in diameter), and (b, d) positions of the maxima of bands, $\lambda_{max}$, and their widths $\Delta\lambda$ for $\lambda$ = (b) 515 and (d) 1030 nm as functions of $N$.

$$\alpha = \frac{\varepsilon(\lambda) - \varepsilon_d}{\varepsilon(\lambda) + 2\varepsilon_d} r^3, \quad (3)$$

is the dipole polarisability of nanoparticle; $r$ is the nanoparticle radius; $\varepsilon_d$ is the permittivity of the medium around the nanoparticle; and

$$\varepsilon(\lambda) = \varepsilon_\infty - \frac{1}{\lambda_p^2[1/\lambda^2 + i/(\gamma_p\lambda)]} + \frac{A_j}{\lambda_j} \sum_{j=1,2} \left[ \frac{\exp(i\varphi_j)}{1/\lambda_j - 1/\lambda - i/\gamma_j} + \frac{\exp(-i\varphi_j)}{1/\lambda_j + 1/\lambda + i/\gamma_j} \right] \quad (4)$$

is the permittivity of the nanoparticle material [17]. The wavelength dependence of permittivity $\varepsilon(\lambda)$ was calculated using the following parameters: high-frequency permittivity $\varepsilon_\infty$ = 1.53, plasma wavelength $\lambda_p$ = 145 nm, interband-transition wavelengths $\lambda_1$ = 468 nm and $\lambda_2$ = 331 nm, linewidths of the corresponding interband transitions $\gamma_1$ = 2300 nm and $\gamma_2$ = 940 nm, dimensionless coefficients $A_1$ = 0.94 and $A_2$ = 1.36, and phases $\varphi_1 = \varphi_2 = -\pi/4$. The plasma wave damping coefficient $\gamma_p$ was chosen taking into account the electron scattering from nanoparticle surface [18]; i.e., $\gamma_p$ = 17000 nm + $2.55 \times 10^{-10}(Av_F/d)$, where $A$ is a coefficient depending on the nanoparticle shape and equal to 1.5 s nm, $v_F = 1.39 \times 10^8$ cm s$^{-1}$ is the Fermi velocity for gold, and $d$ is the nanoparticle diameter in cm.

The results of calculating the spectral dependence of the extinction coefficient $\alpha_{ext} = n\sigma_{ext}$ ($n$ is the nanoparticle concentration, $\sigma_{ext} = \sigma_{abs} + \sigma_{scat}$) for $d$ = 10 nm are shown in Figs 3a and 3c. Comparing these results with the experimental extinction spectra $\alpha_m(\lambda)$, one can see that the spectrum of nanoparticles after fragmentation is approximated well by the theoretical dependence. This is in agreement with the obtained size distributions of nanoparticles, which suggest that their size decreases with increasing $N$ and the maximum of the particle size distribution is in range $d$ = 10–15 nm (Fig. 2d). Nevertheless, the experimental spectra are much wider than the theoretical ones, which is indicative of their inhomogeneous broadening caused by polydispersity of the colloidal nanoparticle solution. Based on the calculation results, one can also estimate the nanoparticle concentration after multipulse fragmentation under 515-nm USLPs; this estimation yields $n \approx 2.5 \times 10^{12}$ cm$^{-3}$.

The results of modelling the shift of the maximum of plasmon-resonance dipole mode, taken for isopropyl alcohol from [19], and the results of our experiments are shown in Fig. 4. It can be seen that the mean nanoparticle diameter depends on the number $N$ of absorbed USLPs as $d \propto a^{-bN}$, which is in agreement with the radical decrease (by more than an order of magnitude) in the mean nanoparticle size in the entire range of $N$ (up to $3 \times 10^8$), apparently, because of the disintegration of larger nanoparticles into small fragments during one fragmentation event [7]. On the contrary, the mechanism of continuous photofragmentation of nanoparticles through evaporation of atoms and small clusters (e.g., dimers or trimers) is believed (in view of small changes in nanoparticle size per one USLP) to be related with weaker and, possibly, even nonmonotonic dependence of the particle diameter on $N$ because of the nonmonotonic character of change in the extinction coefficient at $\lambda$ = 515 nm for nanoparticles of different sizes and nonlinear temperature dependence of the evaporation rate. Currently, we are developing a more informative spectral method for observing details of nanoparticle fragmentation, in particular, in different liquids.

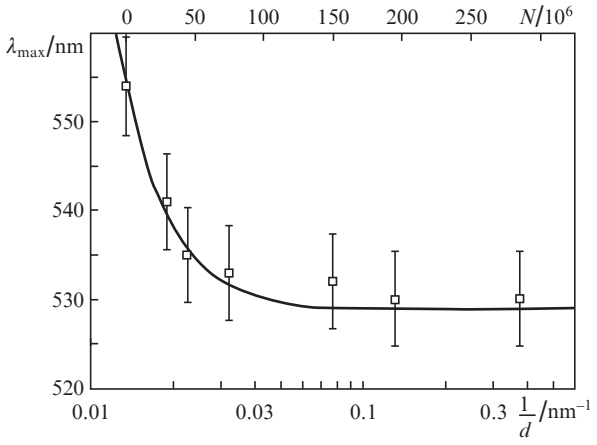


**Figure 4.** Theoretical dependence of the position of the maximum of extinction coefficient $\alpha_{ext}$ (plasmon resonance) $\lambda_{max}$ of a gold nanosphere in a medium with $\varepsilon_d$ = 1.9 on the inverse nanosphere diameter $1/d$ (solid line) and the experimental dependence of the position of the maximum of extinction coefficient $\alpha_m$ on the number of laser pulses $N$ absorbed in the solution (squares).

Finally, the results of calculations based on formulas (1), (3), and (4) show that the absorption cross section at $\lambda$ = 1030 nm for nanoparticles 10–50 nm in diameter is three orders of magnitude smaller than at $\lambda$ = 515 nm. This means that nanoparticle fragmentation under USLPs in the visible range (515 nm) should occur with much higher efficiency; this conclusion was confirmed by our experiments (Figs 2, 3). The transmittance of focused femtosecond laser radiation at $\lambda$ = 515 nm in an unirradiated sample with nanoparticles was found to be ~30% and practically independent of the pulse energy. The corresponding USLP transmittance at $\lambda$ = 1030 nm is much higher – up to 90%.

Thus, we investigated the regime of filamentation-free propagation of USLPs in the IR and visible ranges through a colloidal solution of gold nanoparticles under controlled conditions. The following spectral features of photofragmentation of these nanoparticles were established: high photofragmentation efficiency upon excitation by light with a wavelength close to the plasmon-resonance wavelength of nanoparticles ($\lambda$ = 515 nm) and low photofragmentation efficiency far from this region ($\lambda$ = 1030 nm); these features are in agreement, in particular, with the results of the previous studies with nanosecond laser pulses [3]. Apparently, the effects related to the influence of solvent can manifest themselves only in the mechanism of nanoparticle disintegration into smaller fragments.

## 5. Conclusions

Our experimental study of photofragmentation of colloidal solutions of gold nanoparticles under multipulse irradiation by focused femtosecond laser radiation in IR (1030 nm) and visible (515 nm) ranges in the regime of filamentation-free propagation through the solution revealed high selectivity of photofragmentation in the visible range (under conditions of moderate scattering), which is related to the excitation of plasmon resonance of nanoparticles in the blue spectral wing, in contrast to the regime of close-to-zero photofragmentation

in the IR laser field of comparable intensity, with subsequent stabilisation of the sol of fragmented nanoparticles. The observed exponential decrease of gold nanoparticles in size with an increase in exposure under conditions of femtosecond laser photofragmentation indicates to a greater extent to the disintegration mechanism than to atomic or cluster evaporation.

***Acknowledgements.*** This work was supported in part by the Russian Science Foundation (Grant No. 15-19-00208).

## References

1. Kabashin A.V., Meunier M. *J. Appl. Phys*., **94**, 7941 (2003).
2. Barcikowski S., Hahn A., Kabashin A.V., Chichkov B.N. *Appl. Phys. A*, **87**, 47 (2007).
3. Kirichenko N.A., Sukhov I.A., Shafeev G.A., Shcherbina M.E. *Kvantovaya Elektron*., **42**, 175 (2012) [*Quantum Electron*., **42**, 175 (2012)].
4. Werner D., Hashimoto S. *Langmuir*, **29**, 1295 (2013).
5. Kotaidis V., Dahmen C., von Plessen G., Springer F., Plech A. *J. Chem. Phys*., **124**, 184702 (2006).
6. Werner D., Furube A., Okamoto T., Hashimoto S. *J. Phys. Chem. C*, **115**, 8503 (2011).
7. Hashimoto S., Werner D., Uwada T. *J. Photochem. Photobiol. C*, **13**, 28 (2012).
8. Siems A., Weber S.A.L., Boneberg J., Plech A. *New J. Phys*., **13**, 043018 (2011).
9. Akman E., Oztoprak B.G., Gunes M., Kacar E., Demir A. *Photonics Nanostruct. Fundam. Appl*., **9**, 276 (2011).
10. Sobhan M.A., Ams M., Withford M.J., Goldys E.M. *J. Nanopart. Res*., **12**, 2831 (2010).
11. Ionin A.A., Kudryashov S.I., Makarov S.V., Rudenko A.A., Saltuganov P.N., Seleznev L.V., Sunchugasheva E.S. *Appl. Surf. Sci*., **292**, 678 (2014).
12. Mizeikis V., Juodkazis S., Balciunas T., Misawa H., Kudryashov S.I., Ionin A.A., Zvorykin V.D. *J. Appl. Phys*., **105**, 123106 (2009).
13. Zair A., Guandalini A., Schapper F., Holler M., Biegerti J., Gallmann L., Couairon A., Franco M., Mysyrowicz A., Keller U. *Opt. Express*, **15**, 5394 (2007).
14. Klimov V.V. *Nanoplazmonika* (Nanoplasmonics) (Moscow: Fizmatlit, 2010).
15. Ionin A.A., Kudryashov S.I., Seleznev L.V., Sinitsyn D.V., Bunkin A.F., Lednev V.N., Pershin S.M. *Zh. Eksp. Teor. Fiz*., **143**, 403 (2013).
16. Emel'yanov V.I., Zayarnyi D.A., Ionin A.A., Kiseleva I.V., Kudryashov S.I., Makarov S.V., Rudenko A.A., Nguen Ch.T.Kh. *Pis'ma Zh. Eksp. Teor. Fiz*., **99**, 601 (2014).
17. Etchegoin P.G., Le Ru E.C., Meyer M. *J. Chem. Phys*., **125**, 164705 (2006).
18. Vollmer M., Kreibig U. *Optical Properties of Metal Clusters* (Berlin: Springer, 1995).
19. Myroshnychenko V., Rodríguez-Fernández J., Pastoriza-Santos I., Funston A.M., Novo C., et al. *Chem. Soc. Rev*., **37**, 1792 (2008).